

# Reversible Data Hiding in Encrypted Images Using MSBs Integration and Histogram Modification

Ammar Mohammadi, Mohammad Ali Akhaee and Mansor Nakhkash

**Abstract**— This paper presents a reversible data hiding in an encrypted image that employs based notions of reversible data hiding (RDH) in plain-image including histogram modification and prediction-error computation. In the proposed method, the original image may be encrypted by any desired encryption algorithm. The most significant bit (MSB) of encrypted pixels are integrated to vacate room for embedding data bits. The integrated MSBs will be more robust against failure of reconstruction if they are modified for data embedding. At the recipient, we employ chess-board predictor for lossless reconstruction of the original image thanks to prediction-error analysis. Comparing to existent RDHEI algorithms, not only a separable method to extract data bits is proposed, but also the content-owner may attain a perfect reconstruction of the original image without having data hider's key. Experimental results confirm that the proposed method outperforms state of the art methods.

**Index Terms**—Histogram modification, prediction-errors, reversible data hiding, vacating room after encryption.

## I. INTRODUCTION

Reversible data hiding in plain-image (RDHPI) is drastically developed by many researchers in recent years [1]. In RDHPI, secret data is imperceptibly embedded in a plain-image in a way that the original image can be losslessly recovered after error-free secret data extraction. More presented papers in RDHPI drive from three main notions, namely difference expansion, histogram modification and lossless compression pioneered by [2], [3] and [4], respectively. Some developed studies also employ prediction-error to improve hiding capacity in a determined level of distortion. Attaining more accurate prediction, there exists sharper histogram of errors that can be modified to embed secret data. For example, schemes in [5] and [6] exploit gradient-adjusted prediction (GAP) and median edge detector (MED) predictors introduced in [7] and [8], respectively. Tsai et al. [9] present a predictor, may be denoted as local difference (LD) predictor, that computes difference between pixels intensities in a local area of the image and the most central one to bring out prediction-errors. They embed secret data via histogram modification of the prediction-errors. Sachnev et al. further present cross-dot predictor that divides an image into two “cross” and “dot” sets [10]. Dot set may be predicted using cross one and vice versa. The cross-dot predictor is also represented as a chess-board (CB) predictor in [11].

Besides RDHPI, reversible data hiding in encrypted image (RDHEI) is a solution to preserve privacy for cloud computing/storage services. In RDHEI, there are three parties: image-owner, data hider and recipient. An image-owner may

not trust a channel administrator (or inferior assistant); consequently, the image-owner encrypts the image before uploading to cloud server whereas he/she is not motivated to compress his/her original-content before encryption. On the other side, data hider, i.e. the channel administrator, is not allowed to have the original-content but authorized to embed some handy data in the encrypted image. Therefore, the approach should guarantee lossless original image reconstruction and error-free data extraction at the recipient. These challenges are the cause of developing RDHEI. Schemes introduced in RDHEI may be classified into three categories namely: i) reserving room before encryption (RRBE) [12-19], ii) vacating room by encryption (VRBE) [20-26] and iii) vacating room after encryption (VRAE) [27-32].

In RRBE schemes, there exists a pre-processing before encryption that enables data hider to embed data bits in the encrypted image. Thus, in most RRBE schemes, data hider is not absolutely blind to the original content. On the other hand, most notions in VRBE are realized by encryption of some pixels intensities in a local area of the image using the same cipher byte. This approach preserves correlation between pixels employed to embed data bits. Thus, some information remains disclosed in VRBE. The schemes presented in RRBE and VRBE are separable, which means extraction of the data bits at the recipient is not tied to decrypted information. On the other hand, in joint ones data extraction can be performed just using the decrypted marked image.

In VRAE procedure, data hider is completely blind to original information. After image encryption, data hider vacates rooms to embed data bits without any knowledge of the original-content. Some methods in VRAE are joint [28, 30, 31] while some others are separable [27, 29]. In [32], two different joint and separable procedures are introduced. The separable schemes in VRAE are more functional than joint VRAE schemes; in fact, they are even more functional than RRBE and VRBE schemes. Since data hider is absolutely blind to the original-content, separable VRAE methods preserve the content-owner privacy more than the others. Nevertheless, achieving high embedding capacity is more challengeable in separable VRAE than the others.

From using secret keys point of view, Chen et al. [15] classify three different schemes namely shared independent secret keys (SIK), shared one key (SOK) [15] and shared no secret keys (SNK) [12, 17]. In SIK, there exist two data hider ( $K_d$ ) and image-owner ( $K_e$ ) keys that are shared with recipient independently while in SOK, there exists just one key. In SNK there exists no key to be shared. Most schemes in RDHEI,

including the proposed one, employ SIK to manage secret keys.

Generally, similar to RDHPI, most schemes in RDHEI use the correlation of neighboring pixels in an image and further employ explained notions of RDHPI such as histogram modification, difference expansion, and prediction-error computation. As an example, schemes [15, 17] exploit difference expansion and further, Xiang and Luo employ histogram modification of the prediction-errors to reserve room before encryption [12]. Huang et al. present a new framework in RDHEI that makes it possible to use the most notions of RDH in the plain-image for the encrypted one [24]. In this self-contained scheme, any kind of prediction technique including GAP, MED, CB and LD may be used to estimate prediction-errors.

Schemes [19] and [20] use the based idea of LD predictor to embed data in the encrypted image. They realize a lossless reconstruction (LR) of the original image and error-free extraction of data bits. Also, another scheme employs local correlation of neighboring pixels to reconstruct the original pixel at the recipient [29]. Using MED predictor, Yin et al. allocate some labels for almost all pixels before encryption [14]. Then these labels are compressed via Huffman coding and are embedded along with data bits. They improve [19] and [20] naturally thanks to the source coding algorithms. Fallahpour and Sedaaghi present a RDHPI method that apply the scheme of [3] in non-overlapped blocks of the plain-image to embed data using histogram modification of pixels in a block [33]. In the same approach, Ge et al. introduce a RDHEI method that employs histogram modification ([3]) in non-overlapped blocks of the encrypted image to vacate room for data embedding[25].

As discussed, there exist several schemes in RDHEI that employ based notions of RDHPI to embed data in the encrypted image. Here, we present a new scheme in RDHEI that uses based idea of histogram modification to vacate room after encryption. Data bits are embedded in the integrated MSBs of the target pixels by histogram modification. Target pixels are the ones used for data embedding. In addition, the CB predictor is exploited to perfect reconstruction of the original image at the recipient. Independent secret keys,  $K_e$  and  $K_d$  are used to encrypt the original image and data bits, respectively. In the proposed scheme, not only data bits are perfectly extracted, but also data extraction process is separated from the original image reconstruction. In fact, the proposed scheme can be considered as a functional method which improves the state of the art RDHEI schemes.

The rest of the paper is organized as follows. Related works are discussed in section II. The proposed method is presented in section III including both embedding and error-free extraction of data bits and lossless reconstruction of the original image. Section IV demonstrates the experimental results. Finally, section V concludes the paper.

## II. RELATED WORKS

The proposed scheme is inspired from histogram modification. We employ CB predictor to reconstruct the original image at the recipient by analyzing prediction-error.

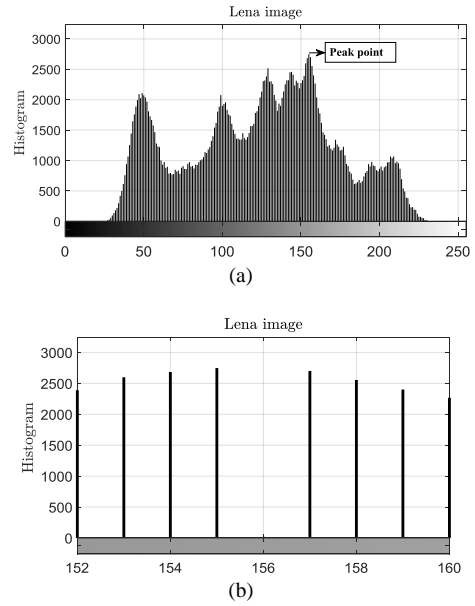


Fig. 1. (a) Histogram of the *Lena* image. (b) Vacate rooms to embed data bits.

For more clarification of the proposed method, we are going to explain the details of these concepts in the following.

### A. Histogram modification

As discussed, Ni et al. [3] present a RDHPI scheme using histogram modification of the original image. In this scheme, they embed data bits in the peak point of the histogram that is the most frequent pixel in the image. Accordingly, they vacate room by histogram modification (VRHM) to provide empty positions used for data embedding. In this way, reversible reconstructing of the original image is possible. For instance, the peak point in the histogram of *Lena* (Fig. 1a) is “155”. Thus, to vacate rooms, all intensities of the image more than “155” are added by 1 (Fig. 1b).

In our proposed procedure, we apply the idea of VRHM in the encrypted image.

### B. Chess-board predictor

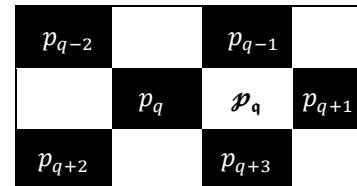


Fig. 2. Part of an image, whose pixels are divided into white and black sections.

The CB predictor, as a non-causal predictor, can provide better prediction than MED and GAP which are considered as the causal predictors. As shown in Fig. 2, in the CB predictor, a black/white pixel may be predicted using its white/black neighbors. For example, prediction of a white pixel  $\tilde{p}_q$  employing its neighboring black ones  $\{p_{q-1}, p_q, p_{q+1}, p_{q+3}\}$  is done by

$$\tilde{p}_q = \lfloor \frac{p_{q-1} + p_q + p_{q+1} + p_{q+3}}{4} \rfloor \quad (1)$$

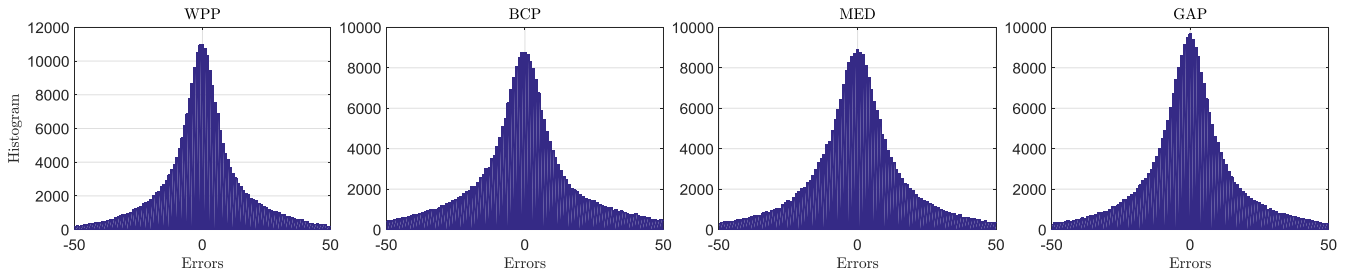


Fig. 3. Histograms of prediction-errors provided by WPP, BCP, MED and GAP predictors for *Baboon* image.

where  $\lfloor \cdot \rfloor$  is the round function. Using  $\tilde{p}_q$  and  $p_q$ , the prediction-error,  $e_q$  is computed by

$$e_q = p_q - \tilde{p}_q \quad (2)$$

More specifically let us denote the prediction of a white pixel by its neighboring black ones as the white plus prediction (WPP). In addition, a central black pixel ( $P_q$ ) can be predicted using its neighboring black ones,  $\{P_{q-2}, P_{q-1}, P_{q+2}, P_{q+3}\}$ , by

$$\tilde{p}_q = \lfloor \frac{P_{q-2} + P_{q-1} + P_{q+2} + P_{q+3}}{4} \rfloor \quad (3)$$

that denoted black cross prediction (BCP). Similarly, in BCP, the prediction-error is calculated by

$$e_q = p_q - \tilde{p}_q \quad (4)$$

### C. Prediction-error analysis

According to (2) or (4), having a prediction-error and a predicted value of an original pixel, the original pixel can be definitely reconstructed. However, as introduced in [19], by having a range of prediction-errors, reconstructing some significant bits of the original pixel is still possible. To be more clarified, let us assume a prediction-error ( $\mathbb{e}$ ) that is computed from subtracting the original pixel ( $p$ ) and its predicted value ( $\mathbb{p}$ ) as:

$$p - \mathbb{p} = \mathbb{e} \quad (5)$$

In [19], it is confirmed that the embedding capacity (EC) will be provided in the MSB of the pixel “ $p$ ”, when the error satisfies

$$|\mathbb{e}| < 64 \quad (6)$$

To gain a better insight, assume a pixel,  $p = p_7 p_6 p_5 p_4 p_3 p_2 p_1 p_0$ , describing eight bits including the LSB,  $p_0$ , to the MSB,  $p_7$ . Having (6),  $p_7$  may be replaced by a data bit in a way that it can be again retrieved at the recipient.

Employing more efficient predictor leads to sharper histogram of the prediction-errors and accordingly provides the more pixels in the image that their prediction-errors satisfy (6). Thus, there exist more MSBs of the pixels to be modified for data embedding.

In Fig. 3, the histograms of prediction-errors provided by

WPP, BCP, MED and GAP predictors are demonstrated for the *Baboon* image. BCP and WPP predictors are applied for all pixels. As shown, WPP provides sensibly a sharper histogram of the prediction-errors than the others. In addition, it seems GAP makes sharper histogram than MED and BCP. Note that pixels whose prediction errors are greater than 64 are not suitable for data embedding since (6) is not satisfied. Let us denote “ $l$ ” as the number of prediction-errors which do not satisfy (6) and “ $L$ ” as the all prediction-errors in an image. Accordingly, we define

$$f_{predictor} = l/L \quad (7)$$

as a probability of failure in reconstructing the reformed MSB of a pixel randomly picked up. Using (7), we have  $f_{WPP} = 0.0017$ ,  $f_{BCP} = 0.021$ ,  $f_{GAP} = 0.014$  and  $f_{MED} = 0.016$  for the *Baboon* image. Although  $f_{WPP}$  is significantly less than the others, there still exists a probability of failure in reconstructing the original pixels. As a solution, we combine several MSBs of target pixels to reduce the risk of failure. Therefore,  $\mathcal{N}$  ones of the MSBs are integrated and the integrated one is used to convey data bit. It can be proved that there exists always a number  $\mathcal{N}$  that can be taken to guarantee perfect reconstruction of the original pixels.

The amount of computed  $f_{pre}$  depends not only upon the kind of the employed predictor, but the type of a host image. The lower the entropy of an image, the lower the probability of the failure can be attained in the recovery process. In other words, generally, smoother images have less  $f_{pre}$ ; despite images like *Baboon*, *Lena* and *F16* result in  $f_{WPP} = 0$ .

As a consequence, we employ WPP predictor in our proposed scheme along with BCP to improve EC.

## III. THE PROPOSED SCHEME

In this section, we introduce the proposed scheme and its stages including image encryption, simple scrambling and unscrambling, embedding and extracting data bits, and recovering the original image.

### A. Image encryption

Encryption of the original image is done using the content-owner secret key,  $K_e$ . Any kind of standard encryption can be used for this purpose. The only restriction is to not changing the positions of the image pixels during encryption. If it occurs, data hider should have knowledge of the new positions to realize the proposed procedure. Therefore, in term of security,

content-owner can chose a desired encryption algorithm.

Regarding  $O$  as the original image, the encrypted image is denoted by  $\hat{O}$ . Let us classify pixels forming  $\hat{O}$  into two groups, namely encrypted white target pixels (EWTPs),  $\{\hat{p}_0, \hat{p}_1, \dots, \hat{p}_q, \dots, \hat{p}_Q\}$  and encrypted black pixels (EBPs),  $\{\hat{p}_0, \hat{p}_1, \dots, \hat{p}_q, \dots, \hat{p}_Q\}$ . The encrypted black pixels are also composed of both encrypted black reference pixels (EBRPs) and encrypted black target pixels (EBTPs). EBRPs remain intact during data embedding process and are used to reconstruct the black or white target pixels at the recipient.

### B. Simple scrambling and unscrambling

Suppose a set  $\mathcal{X} = \{x_0, x_1, \dots, x_q, \dots, x_Q\}$  that is going to be scrambled in a simple way. In this approach,  $\mathcal{X}$  is separated into  $\mathcal{N}$  smaller sets, including  $\frac{Q+1}{\mathcal{N}}$  members, i.e.  $\mathcal{N} \in \mathbb{N}$ . Then, by putting the corresponding members of each set together, the scrambled one  $\mathcal{Y} = \{y_0, y_1, \dots, y_i, \dots, y_Q\}$  is achieved. The number of members in  $\mathcal{X}$  set,  $(Q+1)$ , is selected in such a way that to be divisible by  $\mathcal{N}$ . For instance, regarding  $\mathcal{X} = \{x_0, x_1, x_2, x_3, x_4, x_5\}$  and  $\mathcal{N} = 3$ , by dividing  $\mathcal{X}$  into three smaller sets, we have  $\mathcal{X}_1 = \{x_0, x_1\}$ ,  $\mathcal{X}_2 = \{x_2, x_3\}$  and  $\mathcal{X}_3 = \{x_4, x_5\}$ . The new positions,  $\mathcal{Y} = \{x_0, x_2, x_4, x_1, x_3, x_5\}$ , are achieved by putting the corresponding members of each set together.

Regarding this simple operation, that scrambles  $\mathcal{X}$  to  $\mathcal{Y}$ , in a reverse procedure, the set  $\mathcal{Y}$  is divided into  $\frac{Q+1}{\mathcal{N}}$  smaller ones including  $\mathcal{N}$  members and their corresponding members of each set get together to reversibly give  $\mathcal{X}$ . As an example, considering  $\mathcal{Y} = \{x_0, x_2, x_4, x_1, x_3, x_5\}$  and  $\mathcal{N} = 3$ , we divide  $\mathcal{Y}$  into 2 sets,  $\mathcal{Y}_1 = \{x_0, x_2, x_4\}$  and  $\mathcal{Y}_2 = \{x_1, x_3, x_5\}$ . Putting together corresponding members of these two sets,  $\mathcal{X} = \{x_0, x_1, x_2, x_3, x_4, x_5\}$  is the outcome of this simple unscrambling.

### C. MSB integration, disintegration and data embedding

In this section, we demonstrate the procedure of data embedding in the integrated MSBs of the encrypted pixels. Employing integration, several MSBs must be changed instead of just one MSB to embed data bit that provides more robustness against failure in reconstruction.

This integration is done by assigning a new binary level for  $\mathcal{N}$ -MSBs. It provides an integrated amount less than  $2^{\mathcal{N}}$ . Using histogram modification of the integrated MSBs, some rooms are vacated to implement RDHEL.

Now, assume  $\hat{p}_q = \hat{p}_{(q,7)} \dots \hat{p}_{(q,3)} \dots \hat{p}_{(q,0)}$  as a bitwise

---

Algorithm 1: Shrinking the value of  $m_j$  to  $s_j$  for  $(0 \leq j \leq J)$ .

---

```

for  $j = 0$  to  $J$  do
   $s_j = m_j$ 
  if  $(m_j < 2^{\mathcal{N}-1})$  then
     $s_j = 2^{\mathcal{N}} - 1 - m_j$ 
  end if
end for

```

---



---

Algorithm 2: Embedding data bits.

---

```

for  $j = 0$  to  $J$  do
   $c_j = s_j$ 
  if  $(\hat{d}_j == 1)$  then
     $c_j = |2^{\mathcal{N}} - 1 - s_j|$ 
  end if
end for

```

---

demonstration of an encrypted pixel. As mentioned, when (6) is satisfied for  $p_q, \hat{p}_{(q,7)}$  may be replaced by a bit of data with the ability of perfectly retrievable. Having  $(Q+1)$ -MSBs of the target pixels,  $\hat{\mathcal{P}}_7 = \{\hat{p}_{(0,7)}, \hat{p}_{(1,7)}, \dots, \hat{p}_{(q,7)}, \dots, \hat{p}_{(Q,7)}\}$ , we can describe the process of integration by

$$m_j = \sum_{k=0}^{\mathcal{N}-1} 2^k \times (\hat{p}_{(q-k,7)}), q = \mathcal{N} \times (j+1) - 1, j = 0, 1, \dots, J \quad (8)$$

Thus, integrated MSBs are denoted by  $\mathcal{M} = \{m_0, m_1, \dots, m_j, \dots, m_J\}$ ,  $0 \leq m_j < 2^{\mathcal{N}}, J = \frac{Q-\mathcal{N}+1}{\mathcal{N}}$ .

Regarding the nature of an encrypted image, the histogram of  $\mathcal{M}$  would have the uniform distribution. In order to Embed data bits in  $\mathcal{M}$ , we need to vacate rooms employing the histogram modification of  $\mathcal{M}$ . The approach is a shrinking process that shifts each  $m_j$  less than  $2^{\mathcal{N}-1}$  to a larger one. The shrunken amounts,  $\mathcal{S} = \{s_0, s_1, \dots, s_j, \dots, s_J\}$ ,  $2^{\mathcal{N}-1} \leq s_j < 2^{\mathcal{N}}$ , is achieved using Algorithm 1. In this algorithm, if  $m_j < 2^{\mathcal{N}-1}$ , it is reformed to  $s_j$  which has the most bitwise mutation than  $m_j$ ; in other words,  $m_j$  is replaced with its 1's complement.

Having rooms,  $(J+1)$  bits of encrypted data,  $\hat{\mathcal{D}} = \{\hat{d}_0, \hat{d}_1, \dots, \hat{d}_j, \dots, \hat{d}_J\}$ , encrypted by  $K_d$ , may be embedded in  $\mathcal{S}$  employing Algorithm 2. In this algorithm, to embed an encrypted data bit with value "1" in  $s_j$ , it is replaced by its 1's complement and to embed value "0" it is remained intact.

Let us demonstrate the embedding process with an example. Suppose we have  $\mathcal{N} = 3$  and the integrated values of 27 MSBs, that is  $\mathcal{M} = \{3, 0, 4, 7, 2, 2, 6, 1, 5\}$ . Employing Algorithm 1, vacating rooms is done by shrinking procedure,  $\mathcal{S} = \{4, 7, 4, 7, 5, 5, 6, 6, 5\}$ . In other words, using histogram modification of  $\mathcal{M}$ , changing values between 0 and 3 to others, rooms are vacated to embed  $\hat{\mathcal{D}} = \{1, 1, 0, 1, 0, 0, 1, 0, 1\}$ . Eventually, exploiting Algorithm 2, the carrier set  $\mathcal{C} = \{3, 0, 4, 0, 5, 5, 1, 6, 2\}$ , is achieved. The histogram of  $\mathcal{M}$ ,  $\mathcal{S}$  and  $\mathcal{C}$  are depicted in Fig. 4-a, b and c, respectively.

In order to create a marked encrypted image, first, the set  $\mathcal{C}$  has to be disintegrated using

$$\llbracket \hat{p}_{(\mathcal{N} \times j + k - 1, 7)} \rrbracket = \text{mod} \left( \left\lfloor \frac{c_j}{2^{\mathcal{N}-k}} \right\rfloor, 2 \right), 0 \leq j \leq J, 0 < k \leq \mathcal{N} \quad (9)$$

Consequently, we have marked the encrypted MSBs,  $\llbracket \hat{\mathcal{P}}_7 \rrbracket = \{\llbracket \hat{p}_{(0,7)} \rrbracket, \llbracket \hat{p}_{(1,7)} \rrbracket, \dots, \llbracket \hat{p}_{(q,7)} \rrbracket, \dots, \llbracket \hat{p}_{(Q,7)} \rrbracket\}$ . A marked pixel,

$\llbracket \hat{p}_q \rrbracket$ ,  $q = 0, 1, \dots, Q$ , is created by replacing  $\llbracket \hat{p}_{q,7} \rrbracket$  in the MSB of  $\hat{p}_q$ . Therefore, we have marked EWTPs,  $\llbracket \hat{\mathcal{P}} \rrbracket = \{\llbracket \hat{p}_0 \rrbracket, \llbracket \hat{p}_1 \rrbracket, \dots, \llbracket \hat{p}_q \rrbracket, \dots, \llbracket \hat{p}_Q \rrbracket\}$ .

#### D. Extracting data bits

For data extraction, we just need data hider key,  $K_d$ . Firstly, the MSBs of marked EWTPs as  $\llbracket \hat{\mathcal{P}}_7 \rrbracket$  set are picked up and integrated to recover  $\mathcal{C}$  using (8) where  $(\hat{p}_{(q-k),7})$  and  $m_j$  are replaced respectively by  $\llbracket \hat{p}_{(q-k),7} \rrbracket$  and  $c_j$ ,  $j = 0, 1, \dots, J$ . In this paper, reconstructed sets or pixels are in bold.

Having  $\mathcal{C} = \{c_0, c_1, \dots, c_j, \dots, c_J\}$ , extracting data bits are done employing Algorithm 3. In Algorithm 3,  $j$ 'th bit of the encrypted data,  $\hat{a}_j$ , is extracted using  $c_j$ . Encrypted bits are decrypted using  $K_d$  which result in  $\mathcal{D}$ .

#### E. Recovering the original image

Reconstructing the original image may be initiated by decryption of the marked encrypted image using  $K_e$ . Let us assume  $\mathcal{P}' = \{p'_0, p'_1, \dots, p'_q, \dots, p'_Q\}$  to be the decrypted white target pixels (DWTPs). The subject is to reconstruct the MSBs of DWTPs,  $\mathcal{P}'_7 = \{p'_{0,7}, p'_{1,7}, \dots, p'_{q,7}, \dots, p'_{Q,7}\}$ . Other bits will have been remained intact. The reconstructing process continues by calculating 1's complement of  $\mathcal{P}'_7$  denoted by  $\mathcal{P}''_7 = \{p''_{0,7}, p''_{1,7}, \dots, p''_{q,7}, \dots, p''_{Q,7}\}$ . By replacement of  $\mathcal{P}'_7$  and  $\mathcal{P}''_7$  in the MSB of DWTPs, we have two different candidates of pixels  $\mathcal{P}' = \{p'_0, p'_1, \dots, p'_q, \dots, p'_Q\}$  and  $\mathcal{P}'' = \{p''_0, p''_1, \dots, p''_q, \dots, p''_Q\}$ , respectively. Integrating  $\mathcal{N}$ -prediction-errors, we have a cost function to choose a set of  $\mathcal{N}$ -pixels among these two candidates as the recovered original set. In the following, we demonstrate this procedure in details.

After decryption, the black pixels originally are recovered, because they completely have been remained intact during embedding process. These black pixels are employed to predict pixels of two candidates using (1) where  $p_q$  is replaced by either  $p'_q$  or  $p''_q$ ,  $0 \leq q \leq Q$ . Therefore, having predicted values of pixels for two different candidates, their prediction-errors  $\mathcal{P}'_e = \{e'_0, e'_1, \dots, e'_q, \dots, e'_Q\}$  and  $\mathcal{P}''_e = \{e''_0, e''_1, \dots, e''_q, \dots, e''_Q\}$  may be calculated using (2). In the following, integration of  $\mathcal{N}$  amounts of errors is achieved as an example for  $\mathcal{P}'_e$  by

$$\mathcal{E}'_j = \sum_{k=0}^{\mathcal{N}-1} |e'_{(q-k)}|, q = \mathcal{N} \times (j+1) - 1 \quad (10)$$

Similarly,  $\mathcal{E}''_j$  is attained by (10) for  $\mathcal{P}''_e$  where  $e'_{(q-k)}$  is replaced by  $e''_{(q-k)}$ . The original  $\mathcal{N}$ -pixels belong to either  $\mathcal{P}'$  or  $\mathcal{P}''$  are retrieved by comparing  $\mathcal{E}'_j$  and  $\mathcal{E}''_j$  using Algorithm

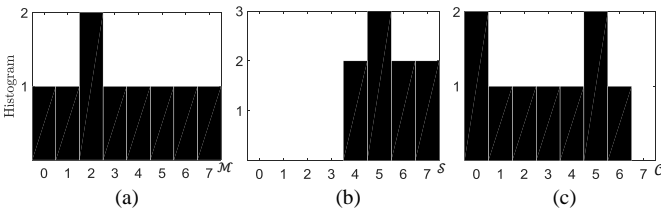


Fig. 4. The histogram of an example of  $\mathcal{M}$ ,  $\mathcal{S}$  and  $\mathcal{C}$  sets.

---

#### Algorithm 3: Extracting data bits.

---

```

for  $j = 0$  to  $J$  do
  if  $(c_j < 2^{\mathcal{N}-1})$  then
     $\hat{a}_j = 1$ 
  else if  $(2^{\mathcal{N}-1} \leq c_j < 2^{\mathcal{N}})$ 
     $\hat{a}_j = 0$ 
  end if
end for

```

---



---

#### Algorithm 4: Reconstructing the original pixels.

---

```

for  $j = 0$  to  $J$  do
   $q = \mathcal{N} \times (j+1) - 1$ 
  if  $(\mathcal{E}''_j \leq \mathcal{E}'_j)$  then
     $\llbracket p_{q-\mathcal{N}+1}, \dots, p_q \rrbracket = \llbracket p''_{q-\mathcal{N}+1}, \dots, p''_q \rrbracket$ 
  else
     $\llbracket p_{q-\mathcal{N}+1}, \dots, p_q \rrbracket = \llbracket p'_{q-\mathcal{N}+1}, \dots, p'_q \rrbracket$ 
  end if
end for

```

---



---

#### Algorithm 5: Risk of LR.

---

```

if  $(\mathcal{R}_j < 16 \times \mathcal{N})$  then
  High risk (HiR)
else if  $(\mathcal{R}_j < 32 \times \mathcal{N})$  then
  Median risk (MeR)
else if  $(\mathcal{R}_j < 64 \times \mathcal{N})$  then
  Low risk (LoR)
else
  Very low risk (VLoR)
end if

```

---

4. Accordingly, for each  $j$ , if  $\mathcal{E}''_j \leq \mathcal{E}'_j$  the recovered  $\mathcal{N}$ -pixels belong to  $\mathcal{P}''$  and vice versa they belong to  $\mathcal{P}'$ . The recovered pixels would be denoted by  $\mathcal{P} = \{p_0, p_1, \dots, p_q, \dots, p_Q\}$ .

Having  $\llbracket p_{q-\mathcal{N}+1}, \dots, p_q \rrbracket = \llbracket p_{q-\mathcal{N}+1}, \dots, p_q \rrbracket$  means  $\mathcal{N}$ -pixels of the original image are losslessly reconstructed. If  $\mathcal{E}'_j$  and  $\mathcal{E}''_j$  are close to each other, it will be a high risk in LR of the original pixels. Therefore, the risk of LR can be analyzed by computing difference between  $\mathcal{E}'_j$  and  $\mathcal{E}''_j$ .

$$\mathcal{R}_j = \left| \mathcal{E}'_j - \mathcal{E}''_j \right| \quad (11)$$

The larger  $\mathcal{R}_j$ , the lower risk of LR would be obtained and vice versa. Employing  $\mathcal{R}_j$  and  $\mathcal{N}$  in Algorithm 5, we can define four classes of risk namely: high risk (HiR), median risk (MeR), low risk (LoR) and very low risk (VLoR). Therefore, in each set of  $\mathcal{N}$ -pixels, we have a risk analysis. The bigger  $\mathcal{N}$  is chosen, the more accurate evaluation of the risk would be realized.

#### F. Overall view of the proposed method

In Fig. 5a, we depict the generic block diagram of the

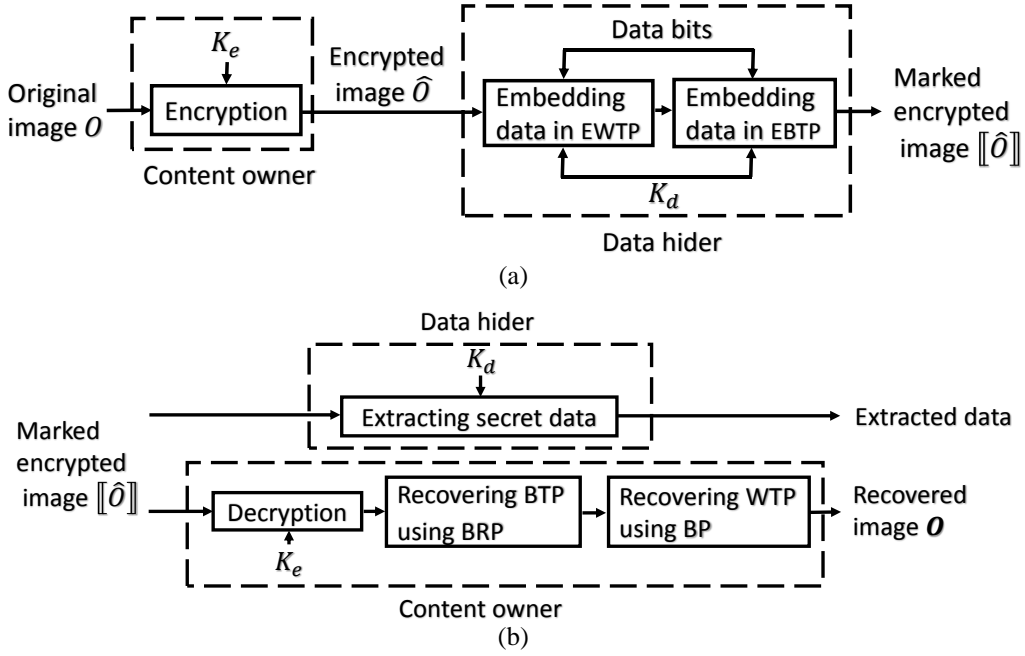


Fig. 5. Generic block diagram of the proposed scheme. (a) Embedding data and forming the marked encrypted image. (b) Extracting data and recovering the original image.

proposed scheme. As shown, embedding is done on EWTP as demonstrated in Subsection C. Then, in a similar way, it can be continued by EBTP,  $\hat{P} = \{\hat{p}_0, \hat{p}_1, \dots, \hat{p}_q, \dots, \hat{p}_Q\}$  to increase EC. In more explanation, by choosing  $N$ -MSBs, the integration can also be performed for  $\hat{P}_7 = \{\hat{p}_{0,7}, \hat{p}_{1,7}, \dots, \hat{p}_{q,7}, \dots, \hat{p}_{Q,7}\}$ .  $N$  is usually considered bigger than  $\mathcal{N}$  because, as discussed, WPP predictor can predict better than BCP one. Thus, integrated MSBs,  $M = \{m_0, m_1, \dots, m_j, \dots, m_J\}$ ,  $0 \leq m_j < 2^N$  and  $J = \frac{Q-N+1}{N}$ , are obtained using (8) where  $m_j$ ,  $p$  and  $\mathcal{N}$  are replaced with  $m_j$ ,  $p$  and  $N$ , respectively. Accordingly, the marked EBTPs,  $[[\hat{P}]] = \{[[\hat{p}_0]], [[\hat{p}_1]], \dots, [[\hat{p}_q]], \dots, [[\hat{p}_Q]]\}$ , are achieved by doing all the steps in Subsection C for  $\hat{P}$ . Eventually, the marked encrypted image, including the marked EWTPs and EBTPs, is created. Meanwhile, BRPs are just encrypted without any more modification. They will be employed to reconstruct other pixels at the recipient. They form 25% of the image.

Now, assuming an original image has the size of  $\mathbb{P} \times \mathbb{Q}$ , by regarding a set of preferred  $\{\mathcal{N}, N\}$  and using all target pixels including black and white ones, EC can be achieved by

$$EC = \mathbb{P} \times \mathbb{Q} \times \left( \frac{1}{2^{\mathcal{N}}} + \frac{1}{4^N} \right) \quad (12)$$

Thus, by choosing  $\{\mathcal{N} = 1, N = 1\}$ , the most possible EC that is  $\frac{3}{4}(\mathbb{P} \times \mathbb{Q})$  would be achieved.

In Fig. 5b, extracting data bits and reconstruction of the original image are described. These two operations can be performed in separable procedures. Extracting data from the marked EBTP,  $[[\hat{P}]]$ , similar to marked EWTP may be done as described in Subsection D.

Reconstructing the original image is initiated by decryption of the marked encrypted image using  $K_e$ . Therefore, BRPs are

completely recovered just by decryption. Using BRPs, BTPs may be retrieved in a similar procedure described in Subsection E except using (3) and (4) instead of (1) and (2) for error prediction. Having black pixels, WTPs are recovered as mentioned in Subsection E. The risk of LR for  $\mathcal{N}/N$ -pixels may be computed during the reconstruction process.

If the MSBs of the target pixels are used sequentially for integration, the MSBs of pixels of rougher regions may have near values. Thus, by scrambling the MSBs, we can reduce the risk of LR at the recipient. In other words, the scrambling prevents integration of MSBs belong to near rough pixels to keep together. Although the scrambling can randomly be performed using  $K_d$ , for the sake of simplicity, we scramble the encrypted MSBs,  $\hat{\mathcal{P}}_7/\hat{P}_7$ , in a simple way (Subsection B). Thus, in more efficient procedure for LR, the scrambled sets are integrated, marked, and finally unscrambled to form the corresponding marked encrypted pixels.

At the recipient, the MSBs of encrypted target pixels are scrambled as well in the same manner for data extraction. Accordingly, at the recipient, to reconstruct the original image, we must scramble the computed prediction-errors. Therefore, in Algorithm 4, we should consider corresponding pixels of the scrambled prediction-errors for reconstructing the original pixels.

#### IV. EXPERIMENTAL RESULT

The performance of the proposed separable VRAE algorithm is evaluated by conducting several experiments. Twelve grayscale images *F16*, *Lena*, *Splash*, *House*, *Boat*, *Elaine*, *Lake*, *Peppers*, *Baboon*, *Stream*, *Aerial* and *APC* from the USC-SIPI database are used as test images. Also, BOWS2 original database, including 10000 grayscale images, are employed to confirm that the proposed algorithm can provide LR of the original image and error-free extraction of data bits. The size of

TABLE I PERFORMANCE ANALYSIS OF THE PROPOSED SCHEME EMPLOYING 12 TEST IMAGES.

Items	images											
	<i>F16</i>	<i>Lena</i>	<i>Splash</i>	<i>House</i>	<i>Boat</i>	<i>Elaine</i>	<i>Lake</i>	<i>Peppers</i>	<i>Baboon</i>	<i>Stream</i>	<i>Aerial</i>	<i>APC</i>
EC (bits)	161290	161290	161290	161290	86021	193548	96774	161290	86021	80645	86021	96774
$\mathcal{N}$	1	1	1	1	2	1	2	1	2	2	2	2
$N$	2	2	2	2	3	1	2	2	3	4	3	2
PSNR	$\infty$	$\infty$	$\infty$	$\infty$	$\infty$	$\infty$	$\infty$	$\infty$	$\infty$	$\infty$	$\infty$	$\infty$
$\mathcal{N}$ -pixels sets	HiR	4	0	0	0	0	0	8	5	0	0	0
	MeR	136	80	4	163	44	27	161	1052	182	130	4
$N$ -pixels sets	HiR	0	0	0	0	0	1	0	13	0	0	0
	MeR	37	9	1	33	68	40	93	35	885	25	103

all test images are  $512 \times 512$ . In experiments, the first and the last two rows and columns of the image are ignored in data embedding process. The peak signal-to-noise ratio (PSNR) is used to estimate the quality of the recovered image. PSNR =  $\infty$  means LR of the original image.

Choosing a set of  $\{\mathcal{N}, N\}$  is somewhat relevant to entropy of an image. The greater the entropy of the image, the greater value of  $\{\mathcal{N}, N\}$  must be selected for LR. However, the more  $\{\mathcal{N}, N\}$  is preferred, the less EC would be achieved. Therefore, there exists a tradeoff between EC and PSNR of the reconstructed image. In Table I, the precise  $\mathcal{N}/N$  for LR of the test images is tabulated. By taking  $\{\mathcal{N} = 1, N = 1\}$  for the *Elaine* image, the most possible EC in the proposed method that is 193548 bits, is achieved. On the other hand, the *Stream* image provides the lowest EC. In this image, the lowest possible  $\mathcal{N}/N$  for LR is  $\{\mathcal{N} = 2, N = 4\}$  that can be regarded for LR of the other test images. Also, in Table I, the risk of LR is evaluated by computing the number of  $\mathcal{N}/N$ -pixels that take either HiR or MeR. Although *F16*, *Peppers* and *Baboon* images are reconstructed perfectly, they include 4, 8 and 5 high risk sets of  $\mathcal{N}$ -pixels, respectively. Also, in reconstructing the sets of  $N$ -pixels, the *Baboon* and *Elaine* images take 13 and 1 sets of high risk, respectively. Accounting the number of HiR and MeR sets, *Baboon* has the most risk of LR; nonetheless, by choosing  $\{\mathcal{N} = 3, N = 5\}$  for data embedding in the *Baboon* image, no set of HiR is left. It is obtained by paying the cost of reducing EC to 55913 bits.

On the other hand, in our scheme, we assume that data hider is completely blind to the original-content; thus, we cannot find out the least possible precise  $\{\mathcal{N}, N\}$  for LR. Nevertheless, in the next subsection, we confirm that a set of  $\{\mathcal{N}, N\}$  may be always found out for LR. It is worth mentioning that in the proposed scheme, error-free extraction of data bits is realized for all test images under any circumstances.

#### A. Lossless retrieval

In Fig. 6, we demonstrate the performance of the proposed scheme in LR and error-free extraction of data bits using 10000 test images of BOWS2 original database. As shown, for various  $\{\mathcal{N}, N\}$ , we accomplished the proposed algorithm to result in the number of failure in LR. For example, in  $\{\mathcal{N} = 3, N = 6\}$ , from 10000 test images, there exist 11 images that are not perfectly reconstructed and consequently the failure rate is  $\mathbb{F}_r = 0.0011$ . As can be seen, the more  $\{\mathcal{N}, N\}$  is preferred, the

less EC and definitely the less failure rate would be achieved. In  $\{\mathcal{N} = 4, N = 6\}$ ,  $\mathbb{F}_r$  is zero. Therefore, there exists permanently a set of  $\{\mathcal{N}, N\}$  to provide LR for all 10000 test images.

As shown in Fig. 6, modifying  $\mathcal{N}$  affects EC and  $\mathbb{F}_r$  more than  $N$ . As an instance, in  $N = 6$ , increasing  $\mathcal{N}$  from two to three decreases EC and  $\mathbb{F}_r$  as much as 21506 bits and 0.0249, respectively; while in  $\mathcal{N} = 3$ , the increment of  $N$  has no noticeable impact on EC and  $\mathbb{F}_r$ . Implementing the proposed algorithm for  $\{\mathcal{N} = 3, N = 6\}$ , we sort all 10000 reconstructed images in the descending order by the number of their HiR  $\mathcal{N}$ -pixels. As discussed, in this implementation, the number of all failures are equal to 11. The first six sorted images are listed in Table II. In this table, PSNR demonstrates four images that are not reconstructed losslessly and thus, four out of all 11 failures include in the first six sorted images. It confirms that the risk analysis is a proper assessment for evaluating LR, i.e. all 11 failures are included in the first 50 sorted images. In any failure, there exist some deformed MSBs that cannot be recovered correctly. The number of deformed MSBs are demonstrated in Table II for various images. The maximum one is just 12 bits for *6501.pgm* image; thus, there is not much bit error rate when LR does not realized.

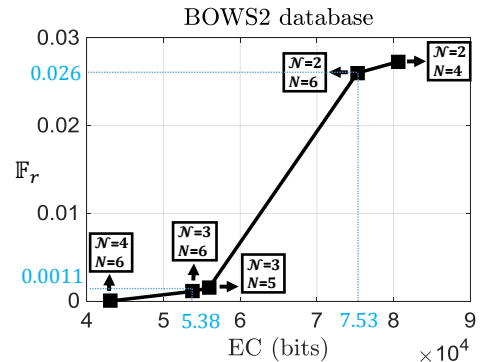


Fig. 6. Efficiency evaluation of the proposed scheme using 10000 test images of Bows2 database in different sets of  $\{\mathcal{N}, N\}$ . We just exploit  $K_e$  to restore the original images. The symbol  $\mathbb{F}_r$  is the failure rate.

TABLE II SIX IMAGES OF BOWS2 ORIGINAL DATABASE THAT HAVE THE MOST NUMBER OF HiR SETS OF  $\mathcal{N}$ -PIXELS.

Items		Images (.pgm)					
		6502	6501	6537	6498	9373	
$\mathcal{N}$ -pixels sets	HiR	15	11	10	6	4	4
	MeR	947	923	778	943	415	460
$\mathcal{N}$ -pixels sets	HiR	1	1	2	1	0	2
	MeR	285	259	413	415	60	170
PSNR		52.39	49.38	$\infty$	52.39	55.4	$\infty$
The number of deformed-MSBs		6	12	0	6	3	0

TABLE III EFFICIENCY COMPARISON BETWEEN THE PROPOSED SCHEME AND OTHER SEPARABLE VRAE ONES FOR NINE TEST IMAGES.

Schemes	Items	images								
		F16	Lena	Splash	House	Boat	Elaine	Lake	Peppers	Baboon
Zhang2012 [27] (CLSB)	EC (bits)	1920	1920	1920	1920	1920	1920	1920	1920	1920
	LR	Pass	Pass	Pass	Pass	Pass	Pass	Pass	Pass	Pass
	LR just by $K_e$	Fail	Fail	Fail	Fail	Fail	Fail	Fail	Fail	Fail
Wu [32]	EC (bits)	<b>130050</b>	<b>130050</b>	<b>130050</b>	<b>130050</b>	<b>130050</b>	<b>130050</b>	<b>130050</b>	<b>130050</b>	<b>130050</b>
	LR	Pass	Pass	Pass	Fail	Fail	Pass	Fail	Fail	Fail
	LR just by $K_e$	Pass	Pass	Pass	Fail	Fail	Pass	Fail	Fail	Fail
Qian [29] (ELDPC)	EC (bits)	77376	77376	77376	77376	77376	77376	77376	77376	77376
	LR	Pass	Pass	Pass	Pass	Pass	Pass	Pass	Pass	Pass
	LR just by $K_e$	Fail	Fail	Fail	Fail	Fail	Fail	Fail	Fail	Fail
Proposed Scheme (HMIMSB)	EC (bits)	<b>86021</b>	<b>86021</b>	<b>86021</b>	<b>86021</b>	<b>86021</b>	<b>86021</b>	<b>86021</b>	<b>86021</b>	<b>86021</b>
	LR	Pass	Pass	Pass	Pass	Pass	Pass	Pass	Pass	Pass
	LR just by $K_e$	Pass	Pass	Pass	Pass	Pass	Pass	Pass	Pass	Pass

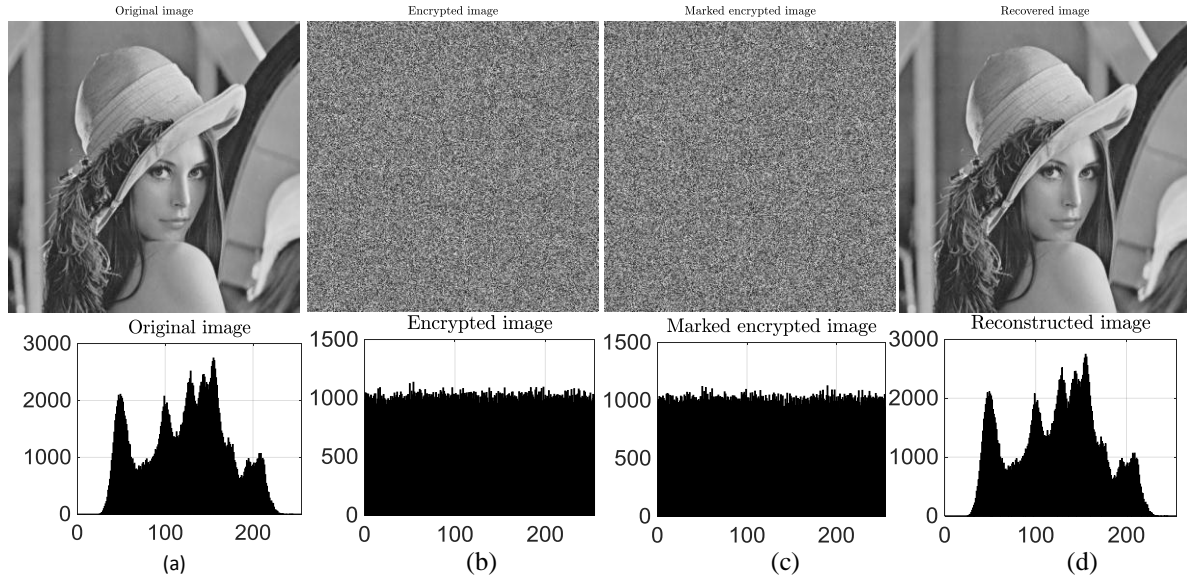


Fig. 7. A visual demonstration of the proposed scheme. (a) Original image. (b) Encrypted image. (c) Marked encrypted image, i.e.  $EC = 161290$  bits. (d) Reconstructed image,  $PSNR = \infty$ . Histogram of the images is also described.

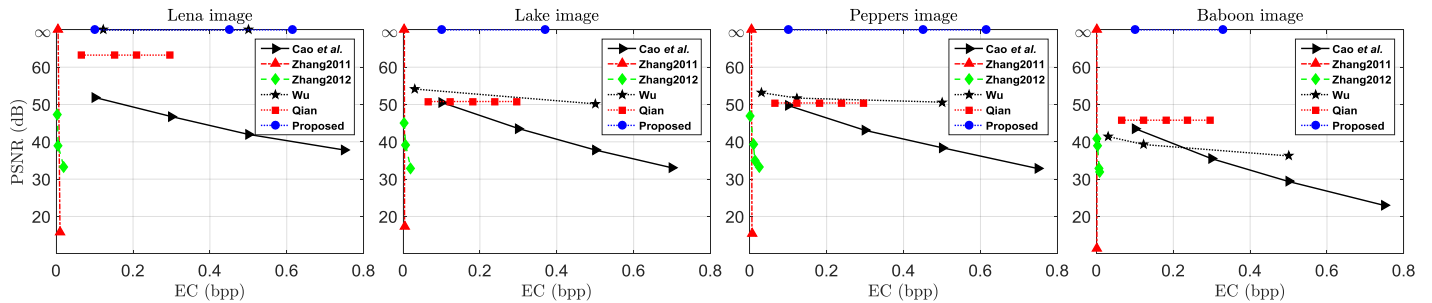


Fig. 8. PSNR comparison of the proposed scheme and other schemes such as Cao et al. [16], Zhang2011[30], Zhang2012 CLSB [27], Qian ELDPC [29], and Wu [32] for four test images.

### B. A visual demonstration of the proposed scheme

Fig. 7 is a visual demonstration of the proposed scheme including the original, encrypted, marked encrypted and

reconstructed images with their depicted histograms, respectively. We optionally employ AES in the counter mode, i.e. a stream cipher procedure, to encrypt the *Lena* test image. As shown in Fig. 7b, after encryption there exist no knowledge of the original image and its content. Due to using a standard encryption algorithm like AES, as can be observed, the histogram of the encrypted image is uniformly distributed which guarantees the security of the proposed algorithm. Since in the proposed scheme, data hider is completely blind to the original-content, it absolutely preserves the content-owner privacy. Moreover, the content-owner can encrypt original-content using any key-based encryption algorithm including stream or block cipher.

Fig. 7c is a description of the marked encrypted image. The histogram still has a uniform distribution. The original image is losslessly reconstructed as shown in Fig. 7d.

### C. Comparison with other schemes

Separable VRAE methods are more functional than the others. The proposed scheme is the only separable VRAE method that makes LR of the original image possible just by having the secret key ( $K_e$ ). We have conducted some experiments to confirm this fact.

In Table III, the proposed scheme is compared with other separable VRAE schemes. After image encryption, the proposed scheme, [27] and [29] vacate room in order by histogram modification of the integrated MSBs (HMIMSB), compresses the least significant bits (CLSB) and encoding using LDPC code (ELDPC). Meanwhile, they employ some parameters that should be used to form a tradeoff between EC and lossless recovery. Their functionality is similar to  $\mathcal{N}/N$ . For a fair comparison between HMIMSB and those of CLSB and ELDPC, we employ these parameters in such a way that all test images are perfectly reconstructed. In this approach, we apply parameters  $\{M = 4, S = 2, L = 271\}$ ,  $\{q = 0.1\}$  for CLSB, ELDPC and  $\{\mathcal{N} = 2, N = 3\}$  for HMIMSB. Note that by choosing less  $L, q$  and  $\mathcal{N}/N$ , both EC and the risk of LR are increased, for all three schemes.

In ELDPC, for LR at the recipient, some information is needed that can be available just by using  $K_d$ . Therefore, as demonstrated in Table III, for this scheme just a high quality version of the original image can be retrieved without having  $K_d$  while in the proposed scheme the original image can be reconstructed perfectly. Besides, HMIMSB can achieve more EC than ELDPC. As described in Table III, in comparison with CLSB, the embedding capacity is significantly improved. Similar to ELDPC, their algorithm is dependent on having  $K_d$  for LR of the original image.

In Wu's scheme [32], using data hider key, they select some target pixels in the encrypted image to embed data bits and employ a predictor such as the modified WPP predictor to reconstruct the original image. Their methods do not guarantee LR, although it may be possible by reducing the number of selected target pixels. In this experiment, we consider the most number of target pixels that may be chosen in Wu's scheme. In this approach, their algorithm fails to perfectly reconstruct the original image for five test images out of nine ones. As

illustrated in Table III, we improve their algorithm by designing a procedure to guarantee LR by employing histogram modification and MSBs integration. However, we pay the cost by less EC. All discussed schemes as well as the proposed scheme provide an error-free data bits extraction

In Fig. 8, the proposed scheme is compared to [16], [27], [29], [30] and [32] in terms of the quality of the reconstructed original image. In this experiment, we suppose schemes [30] and [32] have both encryption and data hider keys while others just have encryption key. In Zhang's method [30], the reconstruction of the original image and extraction of data bits are joint while in our scheme it is separable. In this case, we improve not only EC but also the image quality. To embed data bits, Cao's scheme reserves rooms before encryption using patch-level sparse representation [16]. Generally, the embedding capacity of the proposed scheme is comparable with the Cao's method. However, a preprocessing is allowed before encryption in Cao's scheme while the proposed scheme are absolutely blind to the original-content. As shown in Fig. 8, ELDPC outperforms CLSB and the Cao's scheme in term of PSNR. From LR point of view, our proposed scheme outperform ELDPC. In comparison with Wu's scheme, for *Peppers* and *Lena* images, we reach to higher EC. In *Lake*, *Peppers* and *Baboon* images, they achieve the PSNR of less than 55 dB even by using both keys while in our scheme LR is performed just by  $K_e$ .

## V. CONCLUSION

In this paper, by comparing different predictors, it is demonstrated that WPP is a better choice to reduce the probability of failure in reconstruction of the original image. Moreover, BCP predictor is employed to increase the embedding capacity. By prediction-error analysis, we just choose the MSB of encrypted target pixels for data embedding. These MSBs are integrated to be more robust against failure of reconstruction when they are modified to embed data bits. Employing histogram modification of the integrated MSBs, we vacate rooms for data embedding. At the recipient, data bits are extracted and the original image is reconstructed by separate procedures. We employ the risk analysis to have the probability of LR. The proposed method improves other separable VRAE schemes thanks to using MSBs integration and histogram modification. To the best of our knowledge, we are the only scheme that realizes LR without having  $K_d$ . As a future work, we are willing to improve embedding capacity.

## REFERENCES

- [1] Y.-Q. Shi, X. Li, X. Zhang, H.-T. Wu, and B. Ma, "Reversible data hiding: Advances in the past two decades," *IEEE Access*, vol. 4, pp. 3210-3237, 2016.
- [2] J. Tian, "Reversible data embedding using a difference expansion," *IEEE Transactions on Circuits and Systems for Video Technology*, vol. 13, no. 8, pp. 890-896, Aug. 2003.
- [3] Z. Ni, Y.-Q. Shi, N. Ansari, and W. Su, "Reversible data hiding," *IEEE Transactions on Circuits and Systems for Video Technology*, vol. 16, no. 3, pp. 354-362, Mar. 2006.
- [4] T. Kalker, and F. M. Willems, "Capacity bounds and constructions for reversible data-hiding," in *Proc. International Conference on Digital Signal Processing*, Santorini, Greece, Greece, 2002, pp. 71-76.

- [5] X. Li, W. Zhang, X. Gui, and B. Yang, "A novel reversible data hiding scheme based on two-dimensional difference-histogram modification," *IEEE Transactions on Information Forensics and Security*, vol. 8, no. 7, pp. 1091-1100, Jul. 2013.
- [6] D. M. Thodi, and J. J. Rodríguez, "Expansion embedding techniques for reversible watermarking," *IEEE Transactions on Image Processing*, vol. 16, no. 3, pp. 721-730, Mar. 2007.
- [7] X. Wu, and N. Memon, "Context-based, adaptive, lossless image coding," *IEEE Transactions on Communications*, vol. 45, no. 4, pp. 437 - 444, Apr. 1997.
- [8] M. J. Weinberger, G. Seroussi, and G. Sapiro, "The LOCO-I lossless image compression algorithm: Principles and standardization into JPEG-LS," *IEEE Transactions on Image processing*, vol. 9, no. 8, pp. 1309-1324, Aug. 2000.
- [9] P. Tsai, Y.-C. Hu, and H.-L. Yeh, "Reversible image hiding scheme using predictive coding and histogram shifting," *Signal Processing*, vol. 89, no. 6, pp. 1129-1143, Jun. 2009.
- [10] V. Sachnev, H. J. Kim, J. Nam, S. Suresh, and Y. Q. Shi, "Reversible watermarking algorithm using sorting and prediction," *IEEE Transactions on Circuits and Systems for Video Technology*, vol. 19, no. 7, pp. 989-999, Jul. 2009.
- [11] A. Mohammadi, and M. Nakhkash, "Sorting methods and adaptive thresholding for histogram based reversible data hiding," *arXiv preprint arXiv:1907.05129*, 2019.
- [12] S. Xiang, and X. Luo, "Reversible data hiding in homomorphic encrypted domain by mirroring ciphertext group," *IEEE Transactions on Circuits and Systems for Video Technology*, vol. 28, no. 11, pp. 3099-3110, Nov. 2018.
- [13] K. Ma, W. Zhang, X. Zhao, N. Yu, and F. Li, "Reversible data hiding in encrypted images by reserving room before encryption," *IEEE Transactions on Information Forensics and Security*, vol. 8, no. 3, pp. 553-562, Mar. 2013.
- [14] Z. Yin, Y. Xiang, and X. Zhang, "Reversible data hiding in encrypted images based on multi-MSB prediction and Huffman coding," *IEEE Transactions on Multimedia*, Aug. 2019.
- [15] Y.-C. Chen, T.-H. Hung, S.-H. Hsieh, and C.-W. Shiu, "A new reversible data hiding in encrypted image based on multi-secret sharing and lightweight cryptographic algorithms," *IEEE Transactions on Information Forensics and Security*, vol. 14, no. 12, pp. 3332-3343, Dec. 2019.
- [16] X. Cao, L. Du, X. Wei, D. Meng, and X. Guo, "High capacity reversible data hiding in encrypted images by patch-level sparse representation," *IEEE Transactions on Cybernetics*, vol. 46, no. 5, pp. 1132-1143, May 2016.
- [17] C.-W. Shiu, Y.-C. Chen, and W. Hong, "Encrypted image-based reversible data hiding with public key cryptography from difference expansion," *Signal Processing: Image Communication*, vol. 39, pp. 226-233, Nov. 2015.
- [18] P. Puteaux, and W. Puech, "An efficient MSB prediction-based method for high-capacity reversible data hiding in encrypted images," *IEEE Transactions on Information Forensics and Security*, vol. 13, no. 7, pp. 1670-1681, Jul. 2018.
- [19] A. Mohammadi, and M. Nakhkash, "Reversible data hiding in encrypted images using local difference of neighboring pixels," *arXiv preprint arXiv:1907.05123*, 2019.
- [20] S. Yi, and Y. Zhou, "Separable and reversible data hiding in encrypted images using parametric binary tree labeling," *IEEE Transactions on Multimedia*, vol. 21, no. 1, pp. 51-64, Jan. 2019.
- [21] D. Xu, and R. Wang, "Separable and error-free reversible data hiding in encrypted images," *Signal Processing*, vol. 123, pp. 9-21, Jun. 2016.
- [22] Z. Yin, B. Luo, and W. Hong, "Separable and error-free reversible data hiding in encrypted image with high payload," *The Scientific World Journal*, vol. 2014, Apr. 2014.
- [23] W. Zhang, K. Ma, and N. Yu, "Reversibility improved data hiding in encrypted images," *Signal Processing*, vol. 94, no. 1, pp. 118-127, Jan. 2014.
- [24] F. Huang, J. Huang, and Y.-Q. Shi, "New framework for reversible data hiding in encrypted domain," *IEEE Transactions on Information Forensics and Security*, vol. 11, no. 12, pp. 2777-2789, Dec. 2016.
- [25] H. Ge, Y. Chen, Z. Qian, and J. Wang, "A high capacity multi-level approach for reversible data hiding in encrypted images," *IEEE Transactions on Circuits and Systems for Video Technology*, vol. 29, no. 8, pp. 2285 - 2295, Aug. 2019.
- [26] X. Zhang, "Commutative reversible data hiding and encryption," *Security and Communication Networks*, vol. 6, no. 11, pp. 1396-1403, 2013.
- [27] X. Zhang, "Separable reversible data hiding in encrypted image," *IEEE Transactions on Information Forensics and Security*, vol. 7, no. 2, pp. 826-832, Apr. 2012.
- [28] J. Zhou, W. Sun, L. Dong, X. Liu, O. C. Au, and Y. Y. Tang, "Secure reversible image data hiding over encrypted domain via key modulation," *IEEE Transactions on Circuits and Systems for Video Technology*, vol. 26, no. 3, pp. 441-452, Mar. 2016.
- [29] Z. Qian, and X. Zhang, "Reversible data hiding in encrypted images with distributed source encoding," *IEEE Transactions on Circuits and Systems for Video Technology*, vol. 26, no. 4, pp. 636-646, Apr. 2016.
- [30] X. Zhang, "Reversible data hiding in encrypted image," *IEEE Signal Processing Letters*, vol. 18, no. 4, pp. 255-258, Apr. 2011.
- [31] W. Hong, T.-S. Chen, and H.-Y. Wu, "An improved reversible data hiding in encrypted images using side match," *IEEE Signal Processing Letters*, vol. 19, no. 4, pp. 199-202, Apr. 2012.
- [32] X. Wu, and W. Sun, "High-capacity reversible data hiding in encrypted images by prediction error," *Signal Processing*, vol. 104, pp. 387-400, Nov. 2014.
- [33] M. Fallahpour, and M. H. Sedaaghi, "High capacity lossless data hiding based on histogram modification," *IEICE Electronics Express*, vol. 4, no. 7, pp. 205-210, 2007.